**Aalborg Universitet**



# Simple and effective open switch fault diagnosis of single-phase PWM rectifier

Hu, Keting; Liu, Zhigang; Iannuzzo, Francesco; Blaabjerg, Frede

# Simple and Effective Open Switch Fault Diagnosis of Single-Phase PWM Rectifier

Keting Hu[a] , Zhigang Liu[a,*], Francesco Iannuzzo[b], Frede Blaabjerg[b]

[a] *School of Electrical Engineering, Southwest Jiaotong University, Chengdu, China*
[b] *Department of Energy Technology, Aalborg University, Aalborg, Denmark*

## Abstract

In order to obtain lower harmonics distortion and higher power factors, single-phase pulse-width modulation (PWM) rectifiers are adopted in AC railway drive systems. Therefore, its reliability is of most importance with regards to the safe operation of the train. In this paper, a fault diagnosis method for open switch fault in single-phase PWM rectifier is proposed based on the switching system theory. It requires no additional sensor, nor extra operation states need to be set. Four observers which correspond to four kinds of open switch faults are utilized to detect and locate the faults. Real-time simulations are carried out to validate the effectiveness of this method.

## 1. Introduction

Because of the higher power density and easier maintenance, AC motors have been widely applied in electrical drive systems, including the electrified high-speed railways, hybrid vehicles, etc. To power an AC motor, AC-DC-AC is the most common power supply solution, which consists of a rectifier, a DC-link and an inverter (see Fig. 1). Differently from the conventional diode rectifier, four-quadrant pulse width modulation rectifier (FQPWMR) is adopted in electrified high-speed railways, with the purpose of pursuing higher power factor, lower harmonic distortion and energy recovery [1]. According to [2], however, it is the weakest part of the drive system, which accounts nearly half of the faults from 2009 to 2013 in a Chinese high-speed railway. Therefore, the reliability of FQPWMR is of extreme importance.

Due to the vibration, humidity, high electrical and thermal stress, open-switch fault (OSF) and short-switch fault (SSF) of the Insulated Gate Bipolar Transistor (IGBT) are the most common failures in FQPWMR [3]. On the one hand, the SSF leads to an intense increase of the current, hardware protection is preferred to avoid the catastrophic consequences [4]. On the other hand, in the case of OSF, the system can
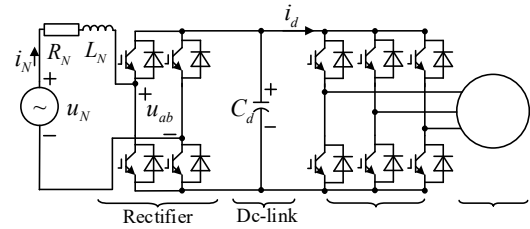


Fig. 1. Schematic of a AC drive system

still run for a while with higher stress on other devices before catastrophic failures occur, which recalls a fast fault diagnosis. At present, most efforts are focused on the three-phase converter, because it has a broad application [5, 6]. Only a few results are reported for OSF in FQPWMR. In [7, 8], it has been pointed out that it is quite challenging to identify the faulty IGBT pairs without additional sensors in single-phase PWM rectifiers. In order to overcome this problem, a particular state has been proposed to be applied to the rectifier for a short time, which can force the detection residual to get different values in case of faulty IGBT [9]. However, such a state can cause catastrophic short-circuit failure if such condition cannot be cleared on time. In [10], PWM pulse driven sampling method is proposed, which decouples the unidentified IGBT pairs on the

Fig. 2 Fault current path under control sequence (a) (0 1 0 1); (b) (1 0 0 1); (c) (1 0 1 0); (d) (0 1 1 0)

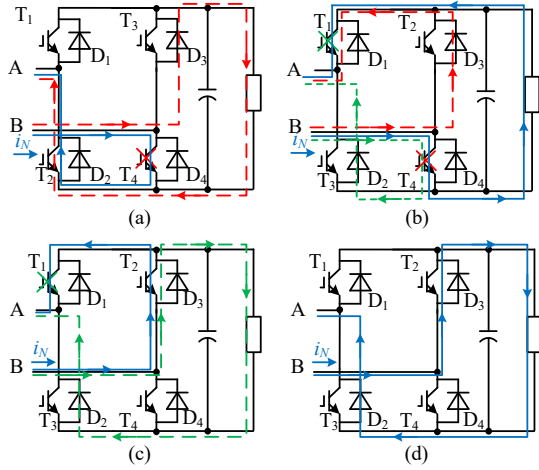modulation level, making it able to distinguish all the four kinds of OSF. However, it is dedicated to the low switching frequency converter.

In this paper, a simple fault-current-observer based diagnosis, which is based on the switching system model (SSM) is proposed. By switching system theory, the grid current can be estimated by an open-loop observer. With the purpose of locating the fault, four fault current observers are generated, which can estimate the fault current under each fault by changing the control sequence of the SSM. When one of the estimated fault currents approaches the measured grid current, the faulty IGBT can be located without additional sensors or specific switching sequence.

## 2. Open switch fault analysis

Taking $T_1$ OSF and $T_4$ OSF as an example to illustrate how the OSFs effect the rectifier operation, and why the two IGBT pairs are challenging to be decoupled. Assume the grid current is positive when it flows into the rectifier and negative in the opposite direction. When the grid current is positive, it flows though the free-wheeling diodes $D_1$ and $D_4$ instead of the two corresponding IGBTs. Thus, the OSFs of $T_1$ and $T_4$ have no impacts on the converter.

When the grid current is negative, the current path is shown in Fig. 2. With the control sequence (0 1 1 0), the current path is same with the one under positive current situation, which indicates that the impacts of $T_1$ and $T_4$ OSFs on the rectifier is negligible. When the control sequence is (0 1 0 1),
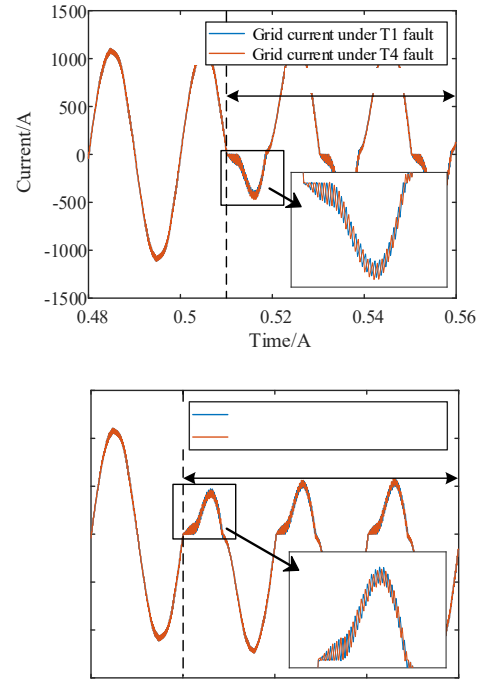


Fig. 3 Fault grid current under (a) $T_1$ and $T_4$ fault; (b) $T_2$ and $T_3$ fault

the current flows through $T_4$ and $D_2$ ( see Fig. 2 (a)). As such, the voltage source is shorted and the current increases. In this case, $T_4$ OSF blocks the current path and it flows through $D_3$ and load, making the current decline. Meanwhile, as the current does not pass through $T_1$, $T_1$ OSF has not impacts on the rectifier. When the control sequence is (1 0 0 1), both $T_1$ and $T_4$ carry currents as Fig. 2 (b) shows. Therefore, either OSF on the two IGBTs will lead to current path change. Under normal condition, the current passes through $T_4$, load and $T_1$, makes both the DC capacitor and the voltage source charge the grid side inductor (see Fig. 1). Thus, the current increases intensely. However, if $T_1$ OSF or $T_4$ OSF occurs, the current will flow through $D_2$ or $D_3$ respectively. Then, there is only the voltage source charge the inductor, which causes the current rises slower. Finally, for the control sequence (1 0 1 0), the current paths before and after the $T_1$ OSF can be seen in Fig. 2 (c). The current decreases under the fault condition instead of rising in the normal condition. Meanwhile, the $T_4$ OSF cannot inflect the rectifier operation.

In overall, the $T_1$ OSF and $T_4$ OSF have the same impacts on the rectifier, which leads to the similar fault current for these two kinds of faults (see Fig. 3 (a)). It is also true for $T_2$ OSF and $T_3$ OSF, and
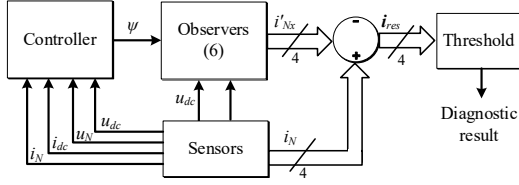
Fig. 4 Diagnostic scheme of the proposed method

the fault currents are shown in Fig. 3 (b). As a consequence, it is difficult to identify the faulty IGBT with only current analysis. In the next section, a simple diagnosis method will be introduced to overcome this problem.

## 3. Proposed diagnosis method

### 3.1. Switching system model

The FQPWMR can be described as

$$di_N/dt = A \times i_N + B_1 \times u_N + B_2 \times u_{ab} \qquad (1)$$

where $A = -R_N/L_N$, $B_1 = 1/L_N$, $B_2 = -1/L_N$, $u_N$ is the grid voltage that can be obtained from the sensors, $R_N$ and $L_N$ are the leakage resistance and the leakage inductance that can be measured. However, the rectifier input voltage $u_{ab}$ cannot be obtained directly. To describe $u_{ab}$, the SSM is introduced. All the operation modes of the rectifier and the corresponding values of $u_{ab}$ are depicted in Table 1. As only three values ($u_{dc}$, 0, $-u_{dc}$) appear in all the modes, equation (1) can be transformed into the SSM as follows

$$di_N/dt = A \cdot i_N + B_1 \cdot u_N + B_\sigma(\psi) \cdot u_{dc}, \ (\sigma \in \{1,2,3\}) \quad (2)$$

where $B_1(\psi)=-1/L_N$, $B_2(\psi)=0$, $B_3(\psi)=-1/L_N$. $B_\sigma(\psi)$ is performed on the system regards of the corresponding operation mode, which is driven by the control sequence

$$\psi = \Phi((\sigma_{k1},\tau_1), (\sigma_{k2},\tau_2),\dots, (\sigma_{k18},\tau_{18})) \qquad (3)$$

where $\sigma_{ki}$ represents the subsystem of one mode and $\tau_i$ is the corresponding working period. As $u_{dc}$ can be sensed and $\psi$ can be obtained from the control system, all the variables of the FQPWMR are known and the system can be described by the SSM.

### 3.2. Fault diagnosis method

With SSM (2), the open-loop grid current

Table 1 The value of $u_{ab}$ under different operation modes

| S1 | S2 | S3 | S4 | $i_N$ | normal | T₁F | T₄F | T₂F | T₃F |
|---|---|---|---|---|---|---|---|---|---|
| 0 | 0 | 0 | 0 | <0 | $-u_{dc}$ | $-u_{dc}$ | $-u_{dc}$ | $-u_{dc}$ | $-u_{dc}$ |
| 0 | 0 | 0 | 0 | >0 | $u_{dc}$ | $u_{dc}$ | $u_{dc}$ | $u_{dc}$ | $u_{dc}$ |
| 0 | 0 | 0 | 1 | <0 | 0 | 0 | $-u_{dc}$ | 0 | 0 |
| 0 | 0 | 0 | 1 | >0 | $u_{dc}$ | $u_{dc}$ | $u_{dc}$ | $u_{dc}$ | $u_{dc}$ |
| 0 | 0 | 1 | 0 | <0 | $-u_{dc}$ | $-u_{dc}$ | $-u_{dc}$ | $-u_{dc}$ | $-u_{dc}$ |
| 0 | 0 | 1 | 0 | >0 | 0 | 0 | 0 | 0 | $u_{dc}$ |
| 0 | 1 | 0 | 0 | <0 | $-u_{dc}$ | $-u_{dc}$ | $-u_{dc}$ | $-u_{dc}$ | $-u_{dc}$ |
| 0 | 1 | 0 | 0 | >0 | 0 | 0 | 0 | $u_{dc}$ | 0 |
| 0 | 1 | 0 | 1 | <0 | 0 | 0 | $-u_{dc}$ | 0 | 0 |
| 0 | 1 | 0 | 1 | >0 | 0 | 0 | 0 | $u_{dc}$ | 0 |
| 0 | 1 | 1 | 0 | <0 | $-u_{dc}$ | $-u_{dc}$ | $-u_{dc}$ | $-u_{dc}$ | $-u_{dc}$ |
| 0 | 1 | 1 | 0 | >0 | $-u_{dc}$ | $-u_{dc}$ | $-u_{dc}$ | 0 | 0 |
| 1 | 0 | 0 | 0 | <0 | 0 | $-u_{dc}$ | 0 | 0 | 0 |
| 1 | 0 | 0 | 0 | >0 | $u_{dc}$ | $u_{dc}$ | $u_{dc}$ | $u_{dc}$ | $u_{dc}$ |
| 1 | 0 | 0 | 1 | <0 | $u_{dc}$ | 0 | 0 | $u_{dc}$ | $u_{dc}$ |
| 1 | 0 | 0 | 1 | >0 | $u_{dc}$ | $u_{dc}$ | $u_{dc}$ | $u_{dc}$ | $u_{dc}$ |
| 1 | 0 | 1 | 0 | <0 | 0 | $-u_{dc}$ | 0 | 0 | 0 |
| 1 | 0 | 1 | 0 | >0 | 0 | 0 | 0 | 0 | $u_{dc}$ |

$T_xF$ – The value of $u_{ab}$ when $T_x$ is faulty

observer can be established as follows

$$di'_N/dt = A \cdot i'_N + B_1 \cdot u_N + B_\sigma(\psi) \cdot u_{dc}, \ (\sigma \in \{1,2,3\}) \quad (4)$$

where $i'_N$ is the observed grid current.

Then, the residual $i_{res}$ can be obtained as Equation (5).

$$i_{res} = i_N - i'_N \qquad (5)$$

However, it is nearly impossible to locate the four kinds of potential faults with one residual which only has two directions, i.e., only two faulty IGBT pairs can be identified. This is another reason for the unidentified IGBT pairs. Aiming at this problem, the fault current observers are introduced. In the observer (4), $B_\sigma$ is driven by $\psi$ that represents the control sequence of the operation modes in Table 1. When an IGBT is open, it is stuck at on state. As a consequence, the control sequence will be changed, i.e. the corresponding command signal is equivalent to off in SSM. For example, if the control sequence is (0 1 0 1) to (**1** 0 0 1) when $T_1$ is faulty, the actual one performed on the system can be treated as (0 1 0 1) to (**0** 0 0 1), and this can be realized in the model by changing the switching sequence. Thus, four fault current observers can be derived as Equation (6), through transforming the normal control sequence into four faulty conditions respectively.

$$di'_{Nx}/dt = A \cdot i'_{Nx} + B_1 \cdot u_N + B_\sigma(\psi_x) \cdot u_{dc}, \ (x \in \{1,2,3,4\}) \quad (6)$$

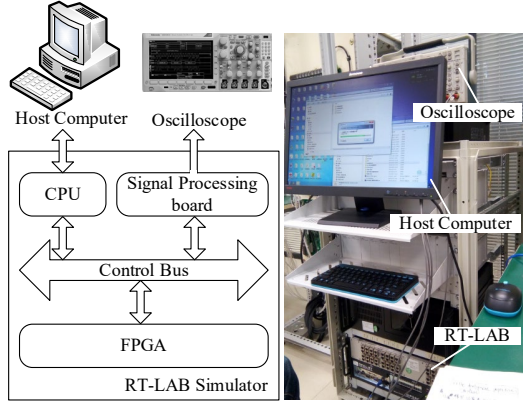Where, $i'_{Nx}$ represents the observed fault current

Fig. 5 Real time simulation platform

under $T_x$ OSF, $B_\sigma(\psi_k)$ denotes the corresponding control sequence under $T_x$ OSF.

With equation (5) and (6), the residual vector that contains four residuals can be derived as follows.

$$\boldsymbol{i}_{res} = [i_{res1}, i_{res2}, i_{res3}, i_{res4}]^{\mathrm{T}} \qquad (7)$$

Each component in residual vector indicates one kind of fault in the rectifier. e.g., $i_{res1}$ is an indicator for $T_1$ fault. If $T_1$ is open, the corresponding observed fault current $i'_{Nx}$ will approach the actual grid current, and the indicator $i_{res1}$ will approach zero, while the irrelevant indicators still remain a relatively large value. Therefore, all the fault conditions can be recognized by $\boldsymbol{i}_{res}$. Considering the modelling error and measurement error, a threshold is adopted to detect the fault, which is set as 500A according to experience. The overall diagnostic scheme is depicted as Fig. 4.

## 4. Real-time simulation

In order to validate the proposed diagnosis method, a real-time simulation is carried out in the RT-lab platform. It consists of a real-time simulator and a host computer, which is shown in Fig. 5. The simulation parameters are given in Table 2. The FQPWMR is controlled by the method presented in [11], while the load is a vector-controlled VSI-fed induction motor. The open-switch fault is emulated by removing the control signal. The $T_1$ fault, $T_2$ fault, $T_3$ fault, and $T_4$ fault are set at 0.5s, 1.5s, 2.5s, and 3.5s respectively and removed at 1s, 2s, 3s and 4s. The real-time simulation results of 125 rad/s speed and 1250 N·m torque, 150 rad/s speed and 1250 N·m torque, 150 rad/s speed and 1000 N·m torque, 125 rad/s speed and 1000 N·m torque of the load induction motor in the drive system are depicted in

Table 2  Simulation parameters

| Parameter | Symbol | Value |
|---|---|---|
| leakage resistance | $R_N$ | 0.13 Ω |
| leakage inductance | $L_N$ | 2.2 mH |
| Dc-link capacitor | $C_d$ | 2 mF |
| RMS grid voltage | $u_N$ | 1550 V |
| Dc-link voltage | $u_{dc}$ | 3000 V |
| Stator resistance | $R_s$ | 0.15 Ω |
| Stator leakage inductance | $L_{ls}$ | 1.42 mH |
| Rotor resistance | $R_r$ | 0.16 Ω |
| Rotor leakage inductance | $L_{lr}$ | 6 mH |
| Mutual inductance | $L_m$ | 25.4 mH |
| Rated voltage | $U_{rate}$ | 2750 V |
| Rated output power | $P_{rate}$ | 560 kW |
| Number of the pole pairs | $n_p$ | 2 |
| Switching frequency | $f_{sw}$ | 2.5 kHz |

Fig. 6 (a), Fig. 6 (b), Fig. 6 (c) and Fig. 6 (d) respectively.

It can be found that the values of all the residuals are more significant than the threshold under normal condition, even the load varies. Under all the different load conditions, the corresponding residual decreases sharply to the value that is smaller than the threshold within 0.03 second when an IGBT OSF occurs, while the remaining residuals stay outside of the residual zone, indicating the faulty IGBT is detected and identified. Though under some load conditions, the irrelevant residual will approach the threshold, its response time is much slower than that of the correct residual. Thus, the potential fault alarm can be eliminated by locking the diagnostic output once the fault is detected and identified.

## 5. Conclusion

An IGBT OCF in FQPWMR has been proposed in this paper. The OSF has been analysed firstly, and the difficulty of identifying the faulty IGBT pairs was explained. Then, the SSM of the rectifier was established, based on which four fault current observers were constructed. Next, by subtracting the real current with the observed current, the residual vector was generated. Finally, the faulty IGBTs were detected and identified through judging if the residuals were lower than the threshold, without additional sensors or particular states. Real-time simulation results validated the effectiveness of this method.
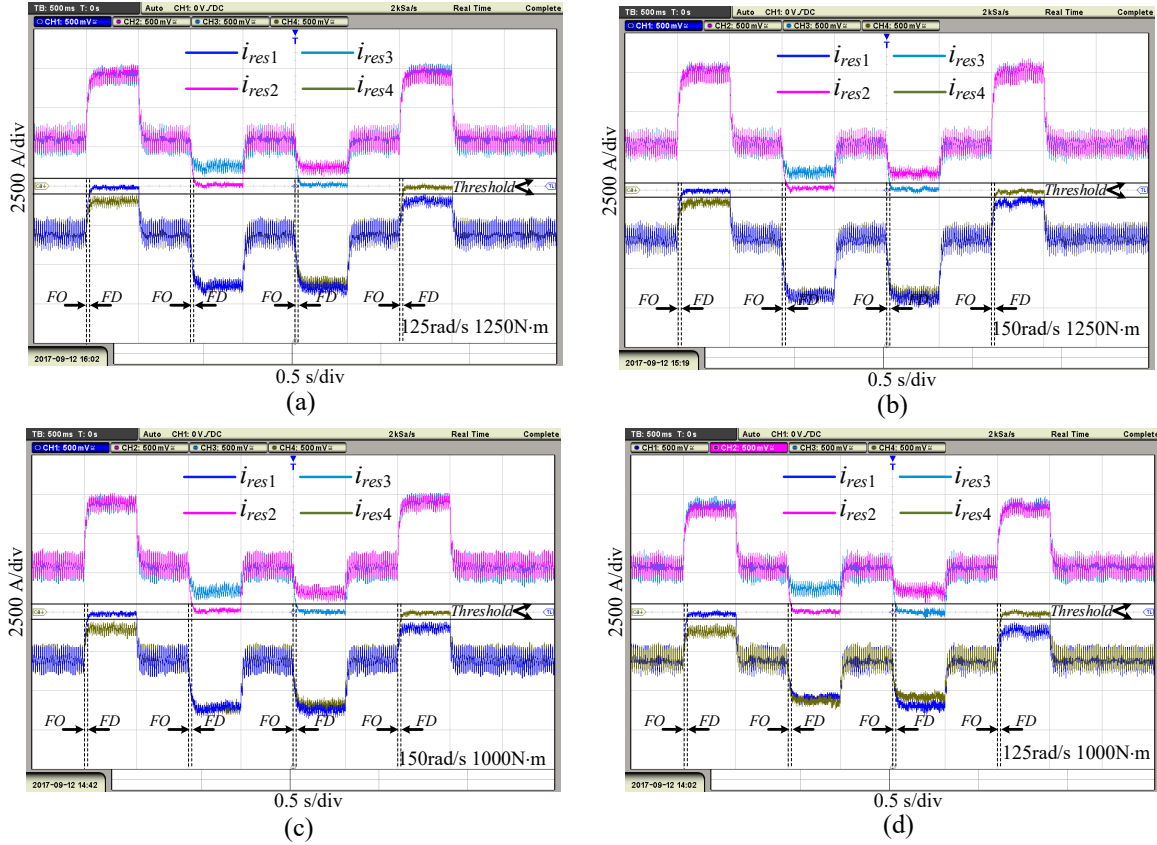
Fig. 6 Residuals when the load of the drive system under (a) 125 rad/s speed and 1250 N·m torque; (b) 150 rad/s speed and 1250 N·m torque; (c) 150 rad/s speed and 1000 N·m torque; (d) 125 rad/s speed and 1000 N·m torque; (FO means fault occurrence and FD indicates fault identified)

## References

[1] A.B. Youssef, S.K. El Khil, I. Slama-Belkhodja. State observer-based sensor fault detection and isolation, and fault tolerant control of a single-phase PWM rectifier for electric railway traction, IEEE Trans. Power Electron. 28(2013) 5842-5853.

[2] B. Gou, Fault diagnosis and fault-tolerant control technology of railway electrical traction converter, Thesis, Southwest Jiaotong University, China, 2016.

[3] S. Yang, A. Bryant, P. Mawby, et al., An industry-based survey of reliability in power electronic converters, IEEE Trans. Ind. Appl. 47 (2011) 1441-1451.

[4] I. Jlassi, J.O. Estima, S.K. El Khil, et al., Multiple open-circuit faults diagnosis in back-to-back converters of PMSG drives for wind turbine systems, IEEE Trans. Power Electron. 30.5 (2015) 2689-2702.

[5] H. Oh, B. Han, P. McCluskey, et al., Physics-of-failure, condition monitoring, and prognostics of insulated gate bipolar transistor modules: A review, IEEE Trans.

Power Electron. 30(2015) 2413-2426.

[6] U. Choi, F Blaabjerg, K. Lee, Study and Handling Methods of Power IGBT Module Failures in Power Electronic Converter Systems, IEEE Trans. Power Electron. 30.5 (2015) 2517-2533.

[7] A.M.S. Mendes, R. F. Rocha, A. J. Marques Cardoso, Analysis of a railway power system based on four quadrant converters operating under faulty conditions, Proc. IEMDC 2011, pp. 1019-1024.

[8] E. Craig, B.C. Mecrow, D.J. Atkinson, A.G. Jack, A fault detection procedure for single phase bridge converters, Proc. Power Electronics and Applications, 1993, pp. 466-471.

[9] B. Gou, X. Ge, S. Wang et al., An Open-Switch Fault Diagnosis Method for Single-Phase PWM Rectifier Using a Model-Based Approach in High-Speed Railway Electrical Traction Drive System, IEEE Trans. Power Electron. 31(2016) 3816-3826.

[10] X. Ge, J. Pu, Y. Liu, Online open-switch fault diagnosis method in single-phase PWM rectifiers, Electron. Lett. 51(2015) 1920-1922.

[11] H. Wang M. Wu, Simulation analysis on low-frequency oscillation in traction power supply system and its suppression method, Power System Technology, 39 (2015) 1088-1095.